



<http://www.diva-portal.org>

Postprint

This is the accepted version of a paper published in *Carbohydrate Research*. This paper has been peer-reviewed but does not include the final publisher proof-corrections or journal pagination.

Citation for the original published paper (version of record):

Rönnols, J., Pendrill, R., Fontana, C., Hamark, C., Angles d'Ortoli, T. et al. (2013)
Complete H-1 and C-13 NMR chemical shift assignments of mono- to tetrasaccharides
as basis for NMR chemical shift predictions of oligosaccharides using the computer
program CASPER
Carbohydrate Research, 380: 156-166
<https://doi.org/10.1016/j.carres.2013.06.026>

Access to the published version may require subscription.

N.B. When citing this work, cite the original published paper.

Permanent link to this version:

<http://urn.kb.se/resolve?urn=urn:nbn:se:su:diva-95416>

Complete ^1H and ^{13}C NMR chemical shift assignments of mono-, di-, and trisaccharides as basis for NMR chemical shift predictions of polysaccharides using the computer program CASPER

Mattias U. Roslund, Elin Säwén, Jens Landström, Jerk Rönnols, K. Hanna M. Jonsson, Magnus Lundborg, Mona V. Svensson and Göran Widmalm*

Department of Organic Chemistry, Arrhenius Laboratory, Stockholm University,
S-106 91 Stockholm, Sweden

*Corresponding author. E-mail: gw@organ.su.se

Abstract

The computer program CASPER uses ^1H and ^{13}C NMR chemical shift data of mono- to trisaccharides for the prediction of chemical shifts of oligo- and polysaccharides. In order to improve the quality of these predictions the ^1H and ^{13}C , as well as ^{31}P when applicable, NMR chemical shifts of 30 mono-, di-, and trisaccharides were assigned. The reducing sugars gave two distinct sets of NMR resonances due to the α - and β -anomeric forms. In total 35 ^1H and ^{13}C NMR chemical shift data sets were obtained from the oligosaccharides. One- and two-dimensional NMR experiments were used for the chemical shift assignments and special techniques were employed in some cases such as 2D $^1\text{H},^{13}\text{C}$ -HSQC Hadamard Transform methodology which was acquired approximately 45 times faster than a regular t_1 incremented $^1\text{H},^{13}\text{C}$ -HSQC experiment and a 1D $^1\text{H},^1\text{H}$ -CSSF-TOCSY experiment which was able to distinguish spin-systems in which the target protons were only 3.3 Hz apart. The ^1H NMR chemical shifts were subsequently refined using total line-shape analysis with the PERCH NMR software. The acquired NMR data were then utilized in the CASPER program (<http://www.casper.organ.su.se/casper/>) for NMR chemical shift predictions of the O-antigen polysaccharides from *Klebsiella* O5, *Shigella flexneri* serotype X, and *Salmonella arizonae* O62. The data were compared to experimental data of the polysaccharides from the two former strains and the lipopolysaccharide of the latter strain showing excellent agreement between predicted and experimental ^1H and ^{13}C NMR chemical shifts.

Keywords: Lipopolysaccharide; Chemical shift prediction; Chemical shift filter; Hadamard matrix.

1. Introduction

NMR spectroscopy has played a key role in the study of polysaccharide structures and functions for the last 30 years. Many polysaccharide repeating-unit structures of bacterial, plant or mammal origin have been published as a result of the development of modern high-field NMR instruments and techniques. NMR is often used to elucidate the structures of both regular and heterogeneous polysaccharides from fungal and plant sources, as well as complex amino-glycans of an animal origin. The combination of the rich structural diversity of oligosaccharides at several levels of complexity and the limited proton chemical shift dispersion ensures that the assignment of NMR resonances and the determination of the solution structure is a demanding task.

A rich diversity of structures originating from more than 100 different monosaccharides and approximately 50 non-sugar components has been identified in bacterial polysaccharides.^{1,2} For mammals the diversity is not as large but even a small number of monosaccharide building blocks can lead to great structural diversity that is complex to analyze and interpret.^{2,3} The variety of possible linkage positions between the monosaccharides adds a further layer of structural complexity to analytical carbohydrate chemistry.

Most naturally occurring monosaccharides have the D-configuration although there are some common exceptions such as L-Fucose and L-Rhamnose. NMR experiment on a monosaccharide in an achiral solvent cannot differentiate between the D- and L-enantiomers, but NMR spectra of diastereomeric derivatives usually allow the absolute configuration to be determined.^{4,5} Most NMR studies of monosaccharides and oligosaccharides involve aqueous solutions in which there is an equilibrium between furanose and pyranose ring forms as well as α - or β -configurations at the anomeric center. As the α - and β -anomers are diastereomeric compounds they are distinguishable and can be assigned by a variety of NMR spectroscopy techniques. The reducing sugars give two distinct sets of NMR resonances due to the α - and β -anomeric forms.

The determination of the linkage position and anomeric configuration, as well as, assigning the monomer stereochemistry is often the primary objective of an NMR study of unknown polysaccharides from biological material. In proton NMR spectroscopy certain structural reporter groups can be used to assign some moieties^{6,7} and the chemical shift region for the anomeric protons can be utilized for assigning the anomeric configuration of various pyranoses. The limited chemical shift range for the non-anomeric protons (usually 3.3 – 4.3 ppm) results in severely overlapping higher-order spectra that makes the signals difficult to use in a straight forward manner for structural investigations. Therefore, the ¹³C NMR signals are more suitable for determination of the glycosylation position, as the resonances from glycosyloxyated carbons are shifted downfield by several ppm in comparison to the monosaccharide unit.⁸ The chemical shift of the anomeric

carbon can also be used for some monosaccharides for assigning the anomeric configuration.⁹ The complexity of these problems has led to the development of computerized approaches.¹⁰⁻¹³ The CASPER program and its database have been continuously improved since the introduction in the late 1980s.^{8,13-16} We here report improvements of ¹H and ¹³C NMR chemical shift predictions made by CASPER based on chemical shift assignments of 30 mono-, di-, and trisaccharides and present the results for NMR chemical shift predictions of three O-antigen polysaccharides.

2. Results and discussion

2.1 Compound selection

The prediction of ¹H and ¹³C NMR chemical shifts by the CASPER program^{13,14} is based on increment rules^{15,16} and as such it relies on the chemical shift information of mono- to trisaccharides in its database. Previously the effects of stereochemical arrangements in oligosaccharides on ¹H and ¹³C NMR chemical shifts were analyzed in detail by synthesizing different combinations of di- and trisaccharides with respect to anomeric α - or β -configuration, absolute configurations of the residues, i.e., D- or L-sugar, and linkage positions.⁸ This approach also made it possible to obtain good approximations of NMR chemical shifts for stereochemical combinations of oligosaccharides that were not present in the database.¹⁴ CASPER utilizes all chemical shifts and chemical shift changes which makes the predictive power high but requires that ¹H and ¹³C NMR chemical shifts of the oligosaccharides in the database are correctly and completely assigned. In the present study we have selected mono-, di- and trisaccharides considered essential based on identification of structural elements present in biological materials in general and in polysaccharides in particular. The compounds investigated are divided into three different parts, viz., monosaccharides, disaccharides and trisaccharides since these are the three subdivisions that CASPER utilizes when NMR chemical shift predictions are performed. We aim to populate the database with sugars for which the NMR assignments are performed at the temperature and pH conditions already established and used by CASPER. A few compounds whose NMR chemical shift assignments are present in the literature¹⁷⁻¹⁹ albeit acquired under different conditions were also included in the present study.

Nine monosaccharides (**1** – **9**) were analyzed (Table 1), three of which were reducing sugars thereby giving two distinct sets of NMR resonances due to the α - and β -anomeric forms. Three key alditols (**1** – **3**) were included since alditol structures are the result of reductive β -eliminations of *O*-glycans from glycoproteins and subsequently analyzed by e.g. ¹H NMR spectroscopy.¹¹ This may also be the modification of choice when anomeric mixtures of the reducing end of an oligosaccharide are to be avoided.²⁰ Two of the monosaccharides were methyl glycosides (**5** and **6**)

and three (**7 – 9**) were carrying substituents. Sixteen disaccharides (**10 – 25**) were investigated (Table 2), one having a glucitol residue (**21**), two with reducing ends giving α - and β -anomeric mixtures (**22** and **23**) and the remaining being methyl glycosides. Of these disaccharides three (**10 – 12**) are 2-substituted, six (**13 – 18**) are 3-substituted, three (**19 – 21**) are 4-substituted, three (**22 – 24**) are 6-substituted and one (**25**) is 7-substituted. These carbohydrate molecules were chosen as models due to the presence of these structural elements in glycoconjugates in general and in polysaccharides in particular. Five trisaccharides (**26 – 30**) were also included (Table 3), one having a hexosaminitol residue (**28**) and the remaining ones being methyl glycosides. As for the disaccharides, the trisaccharides are models for structural elements of bacterial polysaccharides (vide infra).

2.2 Chemical shift assignments

^1H and ^{13}C NMR chemical shift assignments were performed using 1D ^1H and ^{13}C experiments together with a number of 2D $^1\text{H},^1\text{H}$ - and $^1\text{H},^{13}\text{C}$ -correlated experiments. The ^1H NMR chemical shifts were refined using simulation of spectra by total line-shape analysis. $^1\text{H},^1\text{H}$ -correlations were assigned as far as possible using $^1\text{H},^1\text{H}$ -DQF-COSY and/or $^1\text{H},^1\text{H}$ -TOCSY experiments with increasing mixing times from 10 ms up to 120 ms. Long-range correlations over four bonds, in particular H-1 to H-5 correlations in e.g. compounds **4 – 6** and **25** were detected in DQF-COSY and long-range COSY spectra.²¹ One-bond proton-carbon correlations were obtained from $^1\text{H},^{13}\text{C}$ -HSQC and $^1\text{H},^{13}\text{C}$ -HETCOR experiments. Correlations over two and/or three bonds were assigned using $^1\text{H},^{13}\text{C}$ -H2BC and/or $^1\text{H},^{13}\text{C}$ -HMBC experiments. Compounds **10 – 12** were specifically synthesized for this study and the anomeric configurations at the glycosidic linkages were assigned from $^3J_{\text{H}_1,\text{H}_2}$ and/or $^1J_{\text{H}_1,\text{C}_1}$ coupling constants. Linkage positions were ascertained by heteronuclear three-bond correlations over the glycosidic linkages, in particular, for the 2-linked disaccharides. In a few cases, specialized NMR techniques were employed in the assignment process and they are discussed below.

Two-dimensional heteronuclear multi-site Hadamard NMR spectroscopy²² is an efficient way to speed up the acquisition of $^1\text{H},^{13}\text{C}$ -correlated experiments.^{23,24} In a conventional 2D $^1\text{H},^{13}\text{C}$ -HSQC experiment free evolution of the ^{13}C spins take place during the t_1 increment period using typically 256 increments in the indirect F_1 -dimension. When the number of ^{13}C resonances are few and/or cover a relatively large spectral width, the use of a Hadamard transform methodology will be highly advantageous. This approach requires that the ^{13}C resonance frequencies are known in advance, but in the present project we acquire 1D ^{13}C NMR spectra to obtain the chemical shifts of the resonances. Therefore, we already have this information prior to carrying out a $^1\text{H},^{13}\text{C}$ -

correlated experiment. In the 2D Hadamard transform proton-carbon correlated (HSQC-HT) experiment encoding by selective irradiation at the ^{13}C resonance frequencies is carried out according to a suitable Hadamard matrix, typically eight sites ($H-8$) for a monosaccharide or sixteen sites ($H-16$) for a disaccharide where a few excitations are redundant since the number of ^{13}C signals are fewer than the size of the Hadamard matrix. There is no evolution period. Instead, after decoding in the F_1 -dimension by Hadamard transformation and Fourier transformation with respect to t_2 , the 2D spectrum is reconstructed from individual traces. The conventional t_1 incremented 2D $^1\text{H},^{13}\text{C}$ -HSQC spectrum of disaccharide **14** shown for a selected spectral region (Figure 1a) can be compared to the corresponding region of the $^1\text{H},^{13}\text{C}$ -HSQC-HT spectrum (Figure 1b). Two observations can readily be made, viz., (i) the resolution in the F_1 -dimension is lower in the conventional spectrum and (ii) the Hadamard transform spectrum contains a t_1 noise artifact^{25,26} at the proton chemical shift, 3.42 ppm, of the O-methyl group. However, and most importantly, the HSQC-HT experiment was carried out with a speed advantage of a factor of ~ 45 thereby making it a highly advantageous alternative when the number of ^{13}C resonances are relatively few and sufficiently dispersed, as for many disaccharides, monosaccharides or derivatives thereof.²⁷

The complete sets of resonances in the anomeric mixture present for disaccharide **22** were difficult to assign unambiguously. However, the ^1H chemical shifts of the methyl H-6 resonances were different, 1.295 ppm for the major form and 1.290 ppm for the minor form. At a ^1H frequency of 700 MHz, the difference between these two resonances amounts to 3.3 Hz. Selective excitation of the two overlapping doublets is then possible by application of a chemical shift selective filter (CSSF)²⁸ which is a pseudo 2D experiment in which the chemical shift evolution is incremented to a maximum value t_{max} and, when the resulting FIDs are added, the on-resonance magnetizations are constructively added. In contrast, the off-resonance magnetizations, which differ in phase, will destructively interfere, and will be filtered out of the spectrum. A soft pulse is used to excite a narrow spectral region²⁹ and t_{max} is chosen to be equal or longer than $(0.5/\Delta\nu)$ where $\Delta\nu$ is the chemical shift difference between the two overlapping signals. 1D $^1\text{H},^1\text{H}$ -VT-CSSF-TOCSY experiments^{30,31} on disaccharide **22** were carried out using a selective pulse in the spectral region where the H-6 protons of the methyl group of the terminal rhamnose residue in rutinose reside. In two separate experiments using a TOCSY mixing time of 80 ms, the chemical shifts of 1.290 ppm and 1.295 ppm were targeted. Selected regions of the ^1H NMR spectrum of compound **22** are shown in Figure 2a where the different chemical shifts and intensities of the H-6 resonances of the methyl groups are evident. The spectral region between 3.7 and 3.8 ppm shows severe spectral overlap. Using the $^1\text{H},^1\text{H}$ -VT-CSSF-TOCSY experiment the H-3 and H-5 resonances in the minor α -anomeric form (Figure 2b) and the major β -anomeric form (Figure 2c) of **22** are readily assigned.

Trisaccharide **30** has two *N*-acetylated aminosugars in which the ^{13}C chemical shifts of the carbonyl resonances of the *N*-acetyl groups differ by only 0.05 ppm. They were assigned to the corresponding aminosugar by use of a band-selective constant-time heteronuclear multiple-bond correlation ($^1\text{H},^{13}\text{C}$ -BS-CT-HMBC) experiment.³² A ^{13}C -selective pulse is used to select only the narrow carbonyl region of the spectrum, and the use of a constant-time approach suppresses undesirable proton *J*-modulations. In the resulting 2D spectrum the heteronuclear three-bond correlations from the carbonyl groups to the H-2 protons of the aminosugars are observed and also resolved in the indirect F_1 -dimension even though the chemical shift difference is barely 0.05 ppm. A similar example was recently reported for the O-antigen polysaccharide from *E. coli* O82 where the chemical shift difference was only 0.03 ppm between the two carbonyl groups.³³

The ^1H NMR spectral analysis of oligosaccharides is not trivial and spectra are usually severely overlapped even at the high fields currently available. Thus, all chemical shifts and coupling constants cannot be manually extracted. The iterative fitting with the PERCH NMR software^{34,35} provides very accurate spectral parameters for the higher order spectra commonly observed for carbohydrates and only by using computational spectral analyses it was possible to obtain reliable and accurate data. All ^1H NMR chemical shifts were refined by total line-shape analysis using the PERCH NMR software, as exemplified for a selected spectral region of disaccharide **14** (Figure 4) which shows excellent agreement between the experimental spectrum and that obtained by the total line-shape analysis. The ^1H and ^{13}C NMR chemical shifts for **1** – **30** are compiled in Tables 1 – 3. In addition, the ^{31}P NMR chemical shift of monosaccharide **7** and the percentage of α - and β -anomeric forms of the reducing oligosaccharides are also included.

For some of the sugars, NMR chemical shift assignments have been reported in the literature and the agreement between the presently assigned ^1H and ^{13}C NMR chemical shifts is good, e.g., in compounds **1**, **2** and **13**.¹⁷⁻¹⁹ In another case,³⁶ trisaccharide **28**, the ^1H and ^{13}C resonance assignments extended those previously published which contained only partial ^1H chemical shift assignments. However, for the reducing disaccharide **23** with an α/β -anomeric mixture the recently assigned³⁷ ^1H and ^{13}C NMR chemical shifts are not in agreement with our results presented herein; the reason for this discrepancy is unclear. The few cases for which comparisons can be made to literature data in this study show that most assignments are similar although many small chemical shift differences are present and that sometimes deviations are substantial. The accuracy of the NMR chemical shift predictions made by CASPER will not be severely degraded by small deviations due to e.g. slight differences in the experimental conditions, such as assignment of resonances at another temperature from that specified to be used for the database of CASPER.

However, use of incorrect data in the database will degrade CASPER's performance and it is essential to populate the database with high quality data only.

2.3 NMR chemical shift predictions by CASPER

The ^1H and ^{13}C NMR chemical shift data acquired have the effect of increasing the quality of the NMR chemical shift predictions in general and specifically in the cases where a structural element of a mono- to trisaccharide has been missing from the database and approximations of the chemical shifts or glycosylation shifts have been necessary. The updating and improvement of the database is a continuously ongoing process and, when using the web-based version of the CASPER program (<http://www.casper.organ.su.se/casper/>),³⁸ the database will contain the latest information available. Prediction of ^1H and ^{13}C NMR chemical shifts of three O-antigen polysaccharides will exemplify the recent progress, viz., from *Klebsiella* O5, *Shigella flexneri* serotype X, and *Salmonella arizonae* O62 (Figure 5).³⁹⁻⁴² Specifically, trisaccharides **26**, **29** and **30** are related to these polysaccharides, respectively.

The $^1\text{H},^{13}\text{C}$ -HSQC spectrum of the *Klebsiella* O5 polysaccharide is shown in Figure 6a and the $^{13}\text{C}/^1\text{H}$ chemical shifts are given in Table 4. Excellent agreement is present for both ^{13}C and ^1H chemical shifts between experimental data and those predicted from the calculation by CASPER. The assignments of resonances to atoms in different residues are also given. The average absolute deviation was, for ^{13}C chemical shifts, 0.15 ppm/signal, and, for ^1H chemical shifts, 0.02 ppm/signal. The *Klebsiella* O5 polysaccharide contains an unusual terminal α -D-Manp3Me residue³⁹ and the cross-peak of the O-methyl group is observed in the $^1\text{H},^{13}\text{C}$ -HSQC spectrum at $\delta_{\text{H}}/\delta_{\text{C}}$ 3.47/57.26 (Figure 6a). To predict these chemical shifts the substituent effects of the O-methyl group in α -D-Glcp3Me (**8a**) may be used as an approximation. During the course of this work ^1H and ^{13}C NMR assignments of α -D-Manp3Me were reported.⁴³ They were utilized in the NMR chemical shift predictions made by CASPER giving $\delta_{\text{H}}/\delta_{\text{C}}$ 3.45/57.23, in excellent agreement with experimental data for the *Klebsiella* O5 polysaccharide.

The second example is taken from the *Shigella flexneri* serotype X polysaccharide for which ^1H and ^{13}C NMR chemical shifts have been assigned.^{44,45} There is again very close agreement between experimental data and those predicted also leading to assignment of all $^{13}\text{C}/^1\text{H}$ chemical shifts. The average absolute deviation was for ^{13}C chemical shifts, 0.15 ppm/signal, and, for ^1H chemical shifts, 0.03 ppm/signal.

In the third and last example the lipopolysaccharide from *Salmonella arizonae* O62 was analyzed. The quality of the $^1\text{H},^{13}\text{C}$ -HSQC spectrum of the lipopolysaccharide was high (Figure 6b) which made it possible to obtain the chemical shifts directly from the cross-peaks in the

spectrum. The predicted chemical shifts are very close to those observed in the 2D NMR spectrum and assignments to atoms then follow from the calculations made by CASPER. We note, however, a somewhat peculiar observation; at the level chosen to observe cross-peaks in the HSQC spectrum from the O-antigen part of the lipopolysaccharide, one cross-peak predicted to appear at $\delta_{\text{H}}/\delta_{\text{C}}$ 3.93/78.94 (Table 4) was missing, although the signal intensity in the 1D ^{13}C NMR spectrum of the peak at δ_{C} 79.06 was of equal intensity to other signals. Subsequent analysis of the 2D spectrum revealed a cross-peak of lower intensity at $\delta_{\text{H}}/\delta_{\text{C}}$ 3.93/79.06. Thus, if one happens to overlook some of the cross-peaks in 2D spectra, the calculation of anticipated chemical shifts by CASPER still facilitates a detailed analysis when one examines complex NMR spectra. The average absolute deviation was, for ^{13}C chemical shifts, 0.25 ppm/signal, and, for ^1H chemical shifts, 0.04 ppm/signal.

2.4 Conclusions

The assigned ^1H and ^{13}C NMR resonances for **1** – **30** facilitates valuable chemical shift information in cases where models do not exist for CASPER to use in the predictions of chemical shifts of oligo- or polysaccharides. Furthermore, some of the oligosaccharides for which the NMR assignments have been made now make it possible to obtain higher quality predictions with good credibility for the proposed chemical shifts. Less approximations of chemical shifts or chemical shift differences for a given oligosaccharide structure will thus be needed. We have also shown how specialized NMR experiments can be selected and used efficiently to assign ^1H and ^{13}C NMR resonances of oligosaccharides that in general have a low spectral dispersion. The predictive power of CASPER was exemplified by calculating ^1H and ^{13}C chemical shifts of three O-antigen polysaccharides and the agreement with chemical shifts from experimental NMR spectra was shown to be excellent. The approach together with the latest developments⁴⁶ should therefore be possible to use in a large number of carbohydrate applications in which knowledge of ^1H and ^{13}C chemical shifts are required.

3. Experimental

3.1 General

Compounds **1** – **30** were either synthesized at the Department of Organic Chemistry, Arrhenius Laboratory, Stockholm University, or purchased from Sigma-Aldrich, St. Louis, MO, USA, or TCI Europe, Zwijndrecht, Belgium, or Carbosynth, Compton, UK. Additional oligosaccharides were available from previously published studies.⁴⁷⁻⁵¹ Compounds **10** – **12** were synthesized herein using standard methodology;⁵² the anomeric configurations were ascertained from $^3J_{\text{H1,H2}}$ or $^1J_{\text{H1,C1}}$

coupling constants⁵³ and the substitution positions were determined from correlations in ¹H,¹³C-HMBC spectra. The use of D-[1-¹³C]glucitol and D-[6,6'-²H]glucitol aided the assignments of D-glucitol (**2**).

3.2 NMR spectroscopy

¹H and ¹³C NMR chemical shift assignments of all compounds were performed in 5 mm tubes in D₂O with a sample concentration of 6 – 80 mM at 70 °C except otherwise stated. The preparations had pD ≈ 6 for neutral sugars and pD ≈ 8 – 9 for anionic compounds using Na⁺ as a counter ion. Experiments were carried out on five different spectrometers, viz., 400 and 600 MHz Bruker AVANCE spectrometers equipped with inverse probes or broadband probes, 500 and 700 MHz Bruker AVANCE spectrometers equipped TCI Z-Gradient CryoProbes and a 600 MHz Varian INOVA spectrometer equipped with a triple resonance PFG probe. ¹H chemical shifts were referenced to internal sodium 3-trimethylsilyl-(2,2,3,3-²H₄)-propanoate (TSP, δ_H 0.00) using a sweep with of 6 – 8 ppm and ¹³C chemical shifts were referenced to external dioxane in D₂O (δ_C 67.40). The ³¹P chemical shift was referenced to external phosphoric acid (2% H₂PO₄ in D₂O, δ_P 0.00). ¹H assignments were performed using ¹H,¹H-DQF-COSY or ¹H,¹H-TOCSY⁵⁴ experiments recorded over 2 – 5 ppm. For the TOCSY experiments spin-lock strengths of 10 – 15 kHz with five different mixing times ranging from 10 – 120 ms were used. Typically, 2048×256 data points were used in the F₂×F₁ dimensions, respectively, and 8 – 32 scans per t₁ increment were recorded depending on sample concentration and spectrometer sensitivity. When needed, a ¹H,¹³C-H2BC experiment⁵⁵ was recorded with a constant time evolution of 22 ms and processed in the magnitude mode. For the 2D ¹H,¹³C-heteronuclear experiments typically 1024×256 data points were used with 16 – 64 scans per t₁ increment. A spectral width of either 60 or 100 ppm was used for the ¹³C dimension. ¹³C chemical shifts were assigned using three different experiments, namely, coupled and decoupled ¹H,¹³C-HSQC,⁵⁶ ¹³C,¹H-HETCOR or ¹H,¹³C-HSQC-HT²⁴ experiments. Prior to recording of the Hadamard transform (HT) experiment a 1D ¹³C spectrum was recorded and ¹³C frequencies were selected by peak picking. The selected ¹³C frequencies were selectively irradiated by 45 ms 180° Gaussian shaped pulses and were encoded as on or off with a Hadamard matrix using 32 scans. Adiabatic 180° pulses were used for inversion and refocusing on ¹³C. For ¹H decoupling the same pulse length (45 ms) as for the irradiation was used with adiabatic 180° pulses of a 6.5 kHz sweep width. In cases when one-bond ¹H,¹³C-correlations were obtained using a ¹H,¹³C-HSQC experiment and ¹³C NMR chemical shifts differed by <0.1 ppm the ¹³C assignments may be reversed. For assignments of trans-glycosidic correlations ¹H,¹³C-HMBC experiments^{57,58} were recorded with evolution times of 50 – 70 ms for long-range correlations.

^1H chemical shifts were refined iteratively from 1D ^1H spectra both with the integral transform fitting mode and the total line-shape mode of the PERCH NMR iterator PERCHit.^{34,59} Starting values for the iteration were extracted from the experimental 1D and 2D spectra directly. Due to the fact that the line-widths and line-shapes were part of the iterative refinement process of the spectral parameters, the accuracy of the parameters are on the order of the digital resolution.^{35,60} When α/β -ratios are reported sufficiently long ($>5 \times T_1$) relaxation delays were used to ensure correct integration using the PERCH NMR software (PERCH Solutions Ltd., Kuopio, Finland).

The 1D $^1\text{H}, ^1\text{H}$ -VT-CSSF-TOCSY experiments³¹ were performed at 700 MHz with an increment delay $\Delta = 2.8$ ms and 56 increments resulting in a maximum chemical shift evolution interval $t_{\text{max}} = 157$ ms. Two experiments with a mixing time of 80 ms were carried out in which the transmitter frequency offset was set to the chemical shifts of the H-6 resonances of the α - and the β -rhamnosyl residues of compound **22** at 1.290 and 1.295 ppm, respectively. A selective i-SNOB-3 180° pulse⁶¹ with duration of 100 ms and a bandwidth of 27 Hz at 80% height of the excitation profile was used at 700 MHz to single out a narrow spectral region. A DIPSI-2 spin-lock was applied with strength of 11.4 kHz during the isotropic mixing period.

The band-selective, constant-time $^1\text{H}, ^{13}\text{C}$ -HMBC experiment³² employed an initial Δ_1 delay of 50 ms, a selective ^{13}C excitation with a 2.5 ms π Q3 Gaussian cascade pulse, 128 increments over 9 ppm in the F_1 -dimension resulting in a $t_{1(\text{max})}$ of 113 ms.

Acknowledgements

This work was funded by the 6th Research Framework Program of the European Union (Contract: RIDS Contract number 011952) as part of the EUROCarbDB project. It was also supported by grants from the Swedish Research Council, The Knut and Alice Wallenberg Foundation, The Lars Hierta Memorial Foundation, Magn. Bergvall Foundation and Magnus Ehrnrooths Stiftelse (to M.U.R.). We thank Prof. P.-E. Jansson, Prof. S. Oscarson, Prof. R. Ghosh, Prof. Z.-H. Jiang, Dr. E. Maes and Dr. L. A. Mulard for kindly providing oligosaccharides used in this study and Matthias Niemitz for stimulating discussions.

References

1. Lindberg B. In *Polysaccharides*, Dumitriu, S. Ed; Marcel Dekker: New York, 1998; pp 237-273.
2. Adibekian, A.; Stallforth, P.; Hecht, M.-L.; Werz, D. B.; Gagneux, P.; Seeberger, P. H. *Chem. Sci.* **2011**, 2, 337-344.

3. Werz, D. B.; Ranzinger, R.; Herget, S.; Adibekian, A.; von der Lieth, C.-W.; Seeberger, P. H. *ACS Chem. Biol.* **2007**, *2*, 685-691.
4. York, W. S. ; Hantus, S. ; Albersheim, P. ; Darvill, A. G. *Carbohydr. Res.* **1997**, *300*, 199-206.
5. Rao V. S. R.; Qasba P. K.; Balaji P.V.; Chandrasekaran R. *Conformation of Carbohydrates*; Hardwood Academic Publishers, Amsterdam, 1998.
6. Vliegthart, J. F. G.; Dorland, L.; van Halbeek, H. *Adv. Carbohydr. Chem. Biochem.* **1983**, *41*, 209-374.
7. Kamerling, J. P.; Vliegthart, J. F. G. *Biol. Magn. Reson.* **1992**, *10*, 1-194.
8. Söderman, P.; Jansson, P.-E.; Widmalm, G. *J. Chem. Soc., Perkin Trans. 2* **1998**, 639-648.
9. Bock, K.; Pedersen, C. *Adv. Carbohydr. Chem. Biochem.* **1983**, *41*, 27-66.
10. Toukash, F. V.; Shashkov, A. S. *Carbohydr. Res.* **2001**, *335*, 101-114.
11. Maes, E.; Bonachera, F.; Strecker, G.; Guerardel, Y. *Carbohydr. Res.* **2009**, *344*, 322-330.
12. Pereira, F. *Carbohydr. Res.* **2011**, *346*, In Press, Corrected Proof, Available online 23 February 2011.
13. Jansson, P.-E.; Kenne, L.; Widmalm, G. *Carbohydr. Res.* **1987**, *169*, 67-77.
14. Jansson, P.-E.; Kenne, L.; Widmalm, G. *Carbohydr. Res.* **1989**, *188*, 169-191.
15. Jansson, P.-E.; Kenne, L.; Widmalm, G. *Pure & Appl. Chem.* **1989**, *61*, 1181-1192.
16. Stenutz, R. In *Bioinformatics for Glycobiology and Glycomics: an Introduction*. Eds: von der Lieth, C.-W.; Lütke, T.; Frank, M.; John Wiley & Sons, Chichester, UK. 2009. pp 311-320.
17. Franks, F.; Dadok, J.; Ying, S.; Kay, R. L.; Grigera, J. R. *J. Chem. Soc., Faraday Trans.* **1991**, *87*, 579-585.
18. Hoffman, R. E.; Rutherford, T. J.; Mulloy, B.; Davies, D. B. *Magn. Reson. Chem.* **1990**, *28*, 458-464.
19. Pozsgay, V.; Coxon, B. *Carbohydr. Res.* **1995**, *277*, 171-178.
20. Widmalm, G.; Venable, R. M. *Biopolymers* **1994**, *34*, 1079-1088.
21. Bax, A.; Freeman, R. *J. Magn. Reson.* **1981**, *44*, 542-561.
22. Blechta, V.; Freeman, R. *Chem. Phys. Lett.* **1993**, *215*, 341-346.
23. Kupče, Ě.; Freeman, R. *J. Magn. Reson.* **2003**, *163*, 56-63.
24. Kupče, E.; Nishida, T.; Freeman, R. *Prog. Nucl. Magn. Reson. Spectr.* **2003**, *42*, 95-122.
25. Kupče, Ě.; Freeman, R. *J. Magn. Reson.* **2003**, *162*, 158-165.
26. Mehlkopf, A. F.; Korbee, D.; Tiggelman, T. A.; Freeman, R. *J. Magn. Reson.* **1984**, *58*, 315-323.
27. Säwén, E.; Roslund, M. U.; Cumpstey, I.; Widmalm, G. *Carbohydr. Res.* **2010**, *345*, 984-993.
28. Hall, L. D.; Norwood, T. J. *J. Magn. Reson.* **1988**, *76*, 548-554.
29. Hall, L. D.; Norwood, T. J. *J. Magn. Reson.* **1988**, *78*, 582-587.

30. Robinson, P. T.; Pham, T. N.; Uhrín, D. *J. Magn. Reson.* **2004**, *170*, 97-103.
31. Duncan, S. J.; Lewis, R.; Bernstein, M. A.; Sandor, P. *Magn. Reson. Chem.* **2007**, *45*, 283-288.
32. Claridge, T. D. W.; Pérez-Victoria, I. *Org. Biomol. Chem.* **2003**, *1*, 3632-3634.
33. Vilchez, S.; Lundborg, M.; Urbina, F.; Weintraub, A.; Widmalm, G. *Carbohydr. Res.* **2009**, *344*, 2528-2532.
34. Laatikainen, R.; Niemitz M.; Weber U.; Sundelin J.; Hassinen T.; Vepsäläinen, J. *J. Magn. Reson., Ser. A*, **1996**, *120*, 1-10.
35. Laatikainen, R.; Niemitz, M.; Malaisse, W. J.; Biesemans, M.; Willem, R. *Magn. Reson. Med.* **1996**, *36*, 359-365.
36. Florea, D.; Maes, E.; Haddad, M.; Strecker, G. *Biochimie* **2002**, *84*, 611-624.
37. Mazumder, P.; Mukhopadhyay, C. *Carbohydr. Res.* **2010**, *345*, 61-67.
38. Jansson, P.-E.; Stenutz, R.; Widmalm, G. *Carbohydr. Res.* **2006**, *341*, 1003-1010.
39. Jansson, P.-E.; Lönngren, J.; Widmalm, G.; Leontein, K.; Slettengren, K.; Svenson, S. B.; Wrangsell, G.; Dell, A.; Tiller, P. R. *Carbohydr. Res.* **1985**, *145*, 59-66.
40. Kenne, L.; Lindberg, B.; Petersson, K.; Katzenellenbogen, E.; Romanowska, E. *Eur. J. Biochem.* **1977**, *76*, 327-330.
41. Vinogradov, E. V.; Knirel, Y. A.; Kochetkov, N. K.; Schlecht, S.; Mayer, H. *Carbohydr. Res.* **1994**, *253*, 101-110.
42. Olsthoorn, M. M. A.; Petersen, B. O.; Schlecht, S.; Haverkamp, J.; Bock, K.; Thomas-Oates, J. E.; Holst, O. *J. Biol. Chem.* **1998**, *273*, 3817-3829.
43. Reyes Suárez, E.; Kralovec, J. A.; Grindley, T. B. *Carbohydr. Res.* **2010**, *345*, 1190-1204.
44. Jansson, P.-E.; Kenne, L.; Wehler, T. *Carbohydr. Res.* **1988**, *166*, 271-282.
45. Jansson, P.-E.; Kenne, L.; Wehler, T. *Carbohydr. Res.* **1988**, *179*, 359-368.
46. Lundborg, M.; Widmalm, G. *Anal. Chem.* **2011**, *83*, 1514-1517.
47. Garegg, P. J.; Oscarson, S.; Szönyi, M. *Carbohydr. Res.* **1990**, *205*, 125-132.
48. Jiang, Z.-H.; Xu, R.; Wilson, C.; Brenk, A. *Tetrahedr. Lett.* **2007**, *48*, 2915-2918.
49. Maity, S. K.; Maity, S.; Patra, A.; Ghosh, R. *Tetrahedr. Lett.* **2008**, *49*, 5847-5849.
50. Boutet, J.; Guerrerio, C.; Mulard, L. A. *Tetrahedron* **2008**, *64*, 10558-10572.
51. Söderman, P.; Widmalm, G. *Eur. J. Org. Chem.* **2001**, 3453-3456.
52. Osborn, H. M. I. *Carbohydrates*; Academic Press, Amsterdam, 2003.
53. Bundle, D. R.; Lemieux, R. U. *Methods Carbohydr. Chem.* **1976**, *7*, 79-86.
54. Braunschweiler, L.; Ernst, R. R. *J. Magn. Reson.* **1983**, *53*, 521-528.
55. Petersen, B. O.; Vinogradov, E.; Kay, W.; Würtz, P.; Nyberg, N. T.; Duus, J. Ø.; Sørensen, O. W. *Carbohydr. Res.* **2006**, *341*, 550-556.
56. Parella, T.; Sánchez-Ferrando, F.; Virgili, A. *J. Magn. Reson.* **1997**, *126*, 274-277.

57. Bax, A.; Summers, M. F. *J. Am. Chem. Soc.* **1986**, *108*, 2093-2094.
58. Willker, W.; Leibfritz, D.; Kerssebaum, R.; Bermel, W. *Magn. Reson. Chem.* **1993**, *31*, 287-292.
59. Laatikainen, R. *J. Magn. Reson.* **1991**, *92*, 1-9.
60. Roslund, M. U.; Tähtinen, P.; Niemitz, M.; Sjöholm, R. *Carbohydr. Res.* **2008**, *343*, 101-112.
61. Kupče, Ě.; Boyd, J.; Campbell, I. D. *J. Magn. Reson., Ser. B* **1995**, *106*, 300-303.

Figure legends

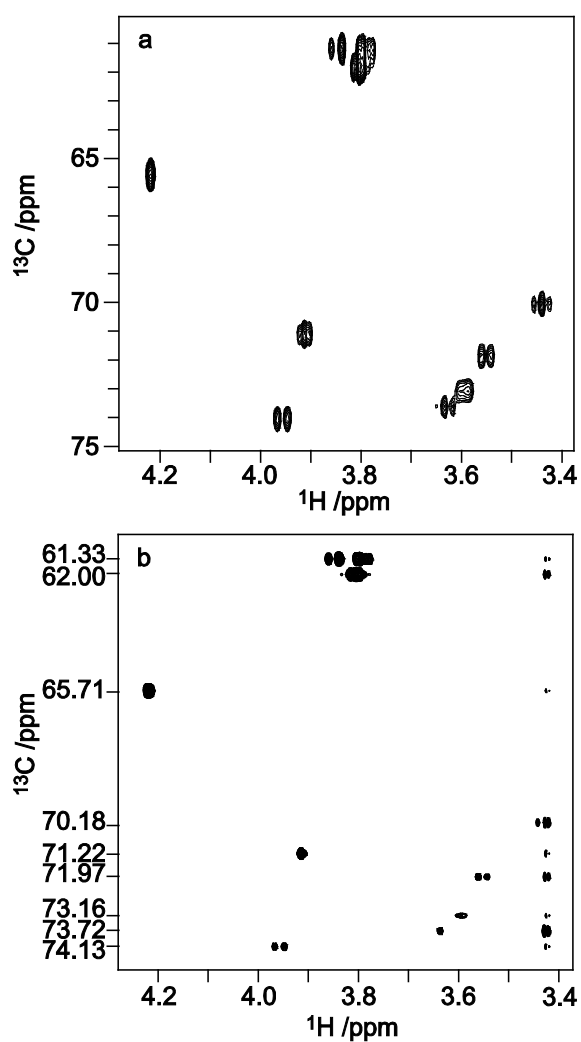


Figure 1. (a) Selected region of the standard t_1 incremented $^1\text{H},^{13}\text{C}$ -HSQC spectrum of α -D-Glcp-(1 \rightarrow 3)- α -D-GalpNAc-OMe (**14**) and (b) the corresponding $^1\text{H},^{13}\text{C}$ -HSQC-Hadamard transform spectrum.

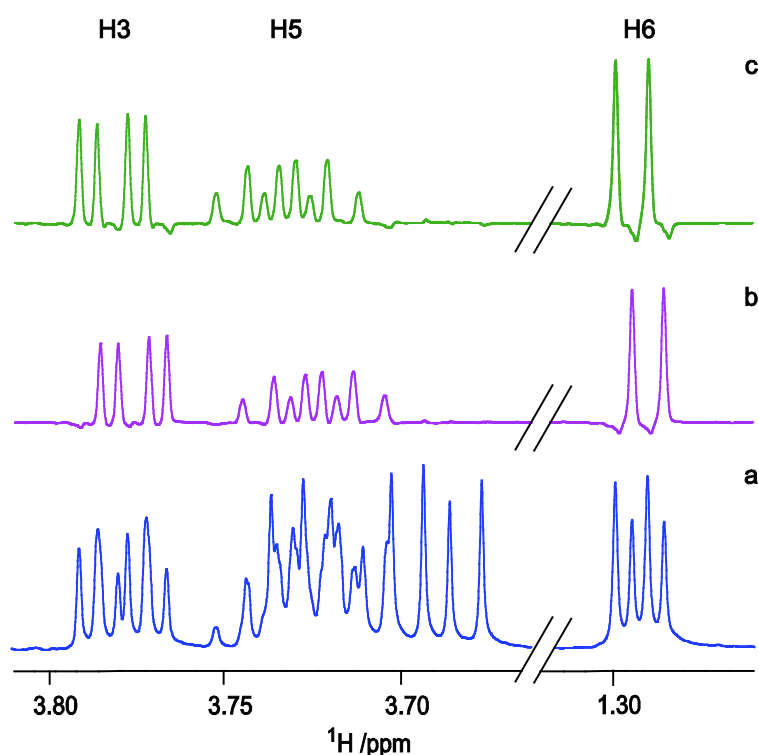


Figure 2. (a) Selected regions of the ^1H NMR spectrum of rutinose, $\alpha\text{-L-Rhap-(1}\rightarrow\text{6)-D-Glcp}$ (**22**); note that the chemical shift scale has been slashed. (b) The corresponding regions of the 1D $^1\text{H},^1\text{H-CSSF-TOCSY}$ spectrum in which the H-6 resonance of rhamnose at 1.290 ppm was targeted. The mixing time used was 80 ms. (c) The corresponding 1D $^1\text{H},^1\text{H-CSSF-TOCSY}$ spectrum in which the H-6 resonance of rhamnose at 1.295 ppm was targeted. The intensities of the H-6 resonances are reduced relative to those from the ring protons.

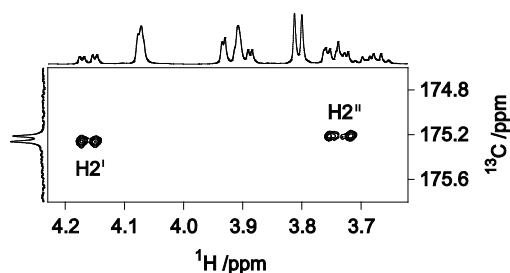


Figure 3. Selected region of the band-selective, constant-time $^1\text{H},^{13}\text{C-HMBC}$ spectrum of trisaccharide $\alpha\text{-D-GalpNAc-(1}\rightarrow\text{2)[}\beta\text{-D-GlcpNAc-(1}\rightarrow\text{3)]-}\alpha\text{-L-Rhap-OMe}$ (**30**) for which the ^{13}C chemical shift difference of the two carbonyl resonances is 0.05 ppm. The three-bond $^1\text{H},^{13}\text{C}$ correlation occurs in the $\alpha\text{-D-GalpNAc}$ residue to the ring proton denoted by H2', and in the $\beta\text{-D-GlcpNAc}$ residue to the ring proton denoted by H2''.

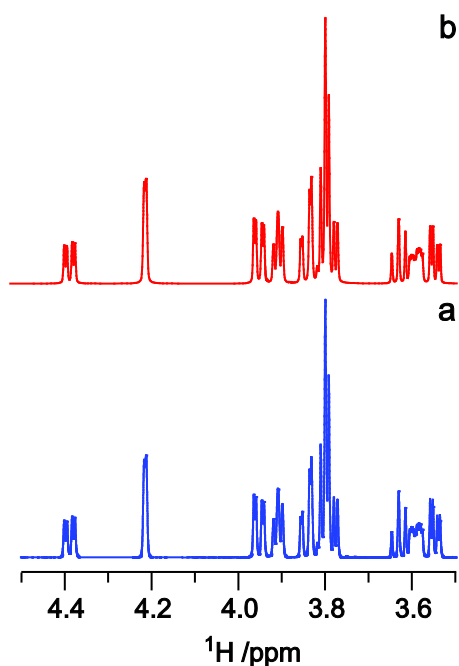


Figure 4. ^1H NMR analysis at 600 MHz of $\alpha\text{-D-Glcp-(1}\rightarrow\text{3)-}\alpha\text{-D-GalpNAc-OMe}$ (**14**): (a) Selected region of the experimental spectrum (blue) and (b) the corresponding simulated spectrum by total-lineshape analysis using the PERCH NMR software (red).

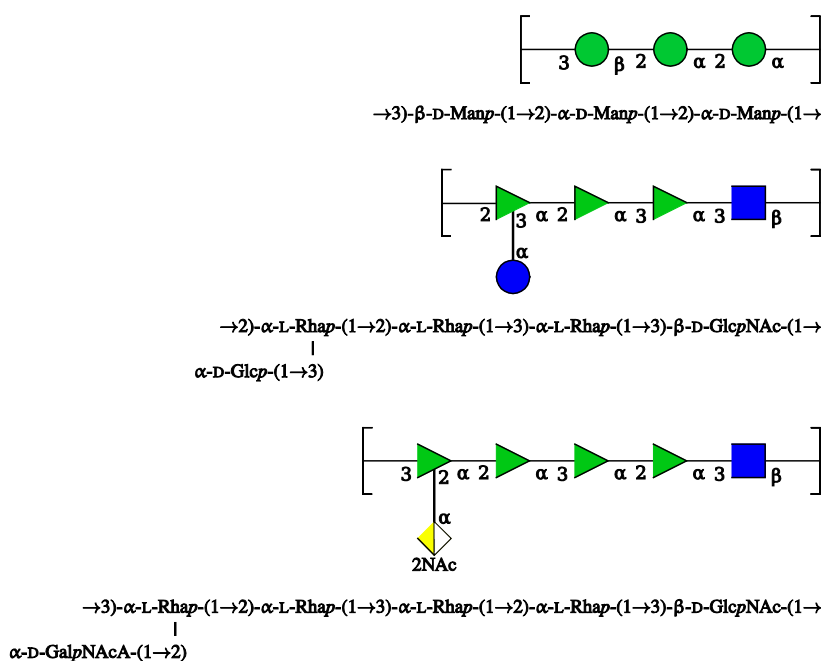


Figure 5. Structure of the repeating units of the O-antigen polysaccharides in CFG-notation and standard nomenclature: (top) *Klebsiella* O5, (middle) *Shigella flexneri* serotype X, and (bottom) *Salmonella arizonae* O62.

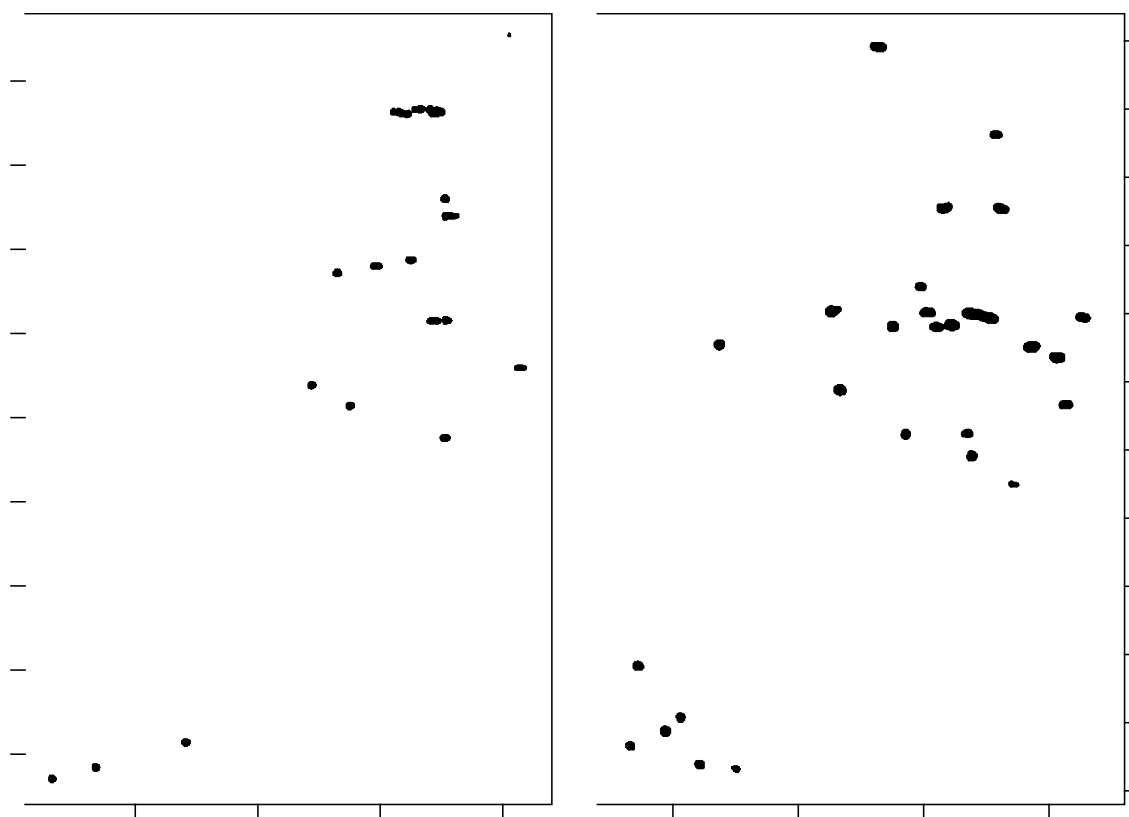


Figure 6. $^1\text{H},^{13}\text{C}$ -HSQC NMR spectra of the polysaccharide from *Klebsiella* O5 recorded at 67 °C (a) and the lipopolysaccharide from *Salmonella arizonae* O62 (b).

Table 1. ¹H, ¹³C, and ³¹P NMR chemical shifts of monosaccharides in D₂O at 70 °C.

Monosaccharide	#	1	2	3	4	5	6	7	OMe	Me	C=O	P	%
D-Xylitol	1	3.655, 3.723 63.57	3.816 72.77	3.660 71.64	3.816 72.77	3.655, 3.723 63.57							
D-Glucitol	2	3.642, 3.737 63.43	3.851 73.67	3.847 70.60	3.689 72.30	3.786 72.18	3.675, 3.826 63.70						
D-GalNAc-ol	3	3.696, 3.749 62.53	4.236 52.51	3.874 69.89	3.442 70.74	3.934 70.99	3.681, 3.682 64.14			2.066 22.80	175.56		
α -D-Xylp	4a	5.178 93.12	3.520 72.41	3.672 73.75	3.605 70.16	3.681, 3.695 61.99							39
β -D-Xylp	4b	4.568 97.53	3.223 75.00	3.433 76.77	3.623 70.27	3.312, 3.927 66.05							61
β -D-Xylp-OMe	5	4.316 104.81	3.270 73.76	3.450 76.62	3.623 70.08	3.323, 3.972 65.92			3.544 57.82				
L- α -D-Hepp-OMe	6	4.745 101.89	3.907 70.82	3.743 71.79	3.838 67.12	3.543 72.10	4.018 69.87	3.704, 3.735 63.94	3.369 55.58				
α -D-Glcp1PO ₃ Na ₂	7	5.472 94.28	3.476 73.23	3.792 74.24	3.394 70.80	3.941 72.82	3.738, 3.872 61.77					2.94	
α -D-Glcp3Me	8a	5.210 92.95	3.590 71.76	3.484 83.43	3.485 69.95	3.833 72.38	3.745, 3.828 61.55			3.613 60.36			42
β -D-Glcp3Me	8b	4.639 96.75	3.308 74.32	3.281 86.09	3.498 69.81	3.456 76.64	3.713, 3.880 61.66			3.613 60.10			58
α -D-Glcp6SO ₃ Na ₂	9a	5.234 93.01	3.560 72.30	3.735 73.57	3.474 70.40	4.021 70.47	4.235, 4.271 68.10						42
β -D-Glcp6SO ₃ Na ₂	9b	4.656 96.86	3.275 74.99	3.506 76.52	3.470 70.34	3.661 74.70	4.193, 4.326 68.10						58

Table 2. ¹H and ¹³C NMR chemical shifts of disaccharides in D₂O at 70 °C.

Disaccharide	#	1	2	3	4	5	6	7	OMe	Me	C=O	%
α -D-Manp-(1→	10	5.143 [172] ^a	4.088	3.897	3.709	4.018	3.807, 3.820					
		102.06	71.01	71.34	67.62	73.41	61.77					
→2)- β -D-Manp-OMe		4.584 [160]	4.113	3.750	3.622	3.398	3.751, 3.936		3.523			
		101.82	76.90	74.48	68.06	77.52	62.11		57.62			
β -D-GlcpNAc-(1→	11	4.764 [165]	3.667	3.600	3.461	3.440	3.764, 3.920			2.056		
		102.04	56.69	74.34	70.82	76.54	61.51			23.20	175.51	
→2)- β -D-Manp-OMe		4.554 [159]	4.166	3.599	3.486	3.353	3.693, 3.920		3.533			
		102.18	78.20	73.01	68.31	77.16	62.29		57.64			
β -L-Fucp-(1→	12	4.466 (7.86) ^b	3.547	3.654	3.762	3.810	1.280					
		102.81	71.28	73.77	72.13	71.93	16.15					
→2)- α -D-Galp-OMe		5.001 (3.82) ^b	4.019	3.917	4.058	3.907	3.774, 3.777		3.435			
		98.44	76.91	68.94	69.87	71.41	61.98		55.71			
α -D-Galp-(1→	13	5.383	3.831	3.779	3.998	3.876	3.734, 3.747					
		100.14	69.43	70.19	69.92	71.64	61.46					
→3)- α -D-GlcpNAc-OMe		4.744	4.061	3.876	3.727	3.687	3.781, 3.869		3.413	2.050		
		99.10	52.73	78.90	71.57	72.35	61.37		55.97	22.89	174.76	
α -D-Glcp-(1→	14	5.084	3.547	3.629	3.437	3.590	3.788, 3.842					
		95.95	71.97	73.72	70.18	73.16	61.33					
→3)- α -D-GalpNAc-OMe		4.792	4.389	3.953	4.215	3.908	3.790, 3.811		3.421	2.047		
		99.18	48.72	74.13	65.71	71.22	62.00		55.99	22.91	174.87	
β -D-Glcp-(1→	15	4.519	3.297	3.462	3.407	3.416	3.723, 3.874					
		104.75	73.95	76.63	70.50	76.68	61.63					
→3)- α -D-GalpNAc-OMe		4.789	4.334	3.973	4.208	3.921	3.752, 3.772		3.398	2.019		
		99.26	49.46	78.34	69.46	71.30	62.07		56.08	22.96	175.32	
α -L-Fucp-(1→	16	5.015	3.722	3.879	3.818	4.140	1.216					
		101.65	69.04	70.38	72.56	67.85	16.01					
→3)- α -D-GalpNAc-OMe		4.799	4.369	3.894	4.043	3.938	3.763, 3.788		3.418	2.029		
		99.18	49.48	77.00	69.04	71.45	61.89		56.00	22.84	175.38	
β -L-Fucp-(1→	17	4.441	3.494	3.640	3.745	3.766	1.293					
		101.86	71.37	73.82	72.22	71.76	16.34					
→3)- α -D-GalpNAc-OMe		4.914	4.222	4.031	4.191	3.890	3.782, 3.801		3.404	2.040		
		98.94	49.45	76.12	67.17	71.39	62.02		56.04	23.09	175.26	
β -D-Galp-(1→	18	4.649	3.614	3.681	3.944	3.722	3.772, 3.796					
		104.10	72.12	73.53	69.48	76.14	61.82					
→3)- β -D-Glcp-OMe		4.408	3.478	3.746	3.517	3.489	3.747, 3.926		3.578			
		103.81	73.44	85.81	69.22	76.36	61.74		57.88			

β -D-Galp-(1→	19	4.462	3.570	3.667	3.950	3.728	3.776, 3.803		
		103.81	71.89	73.58	69.49	76.16	61.81		
→4)- β -D-Glcp-OMe		4.397	3.331	3.659	3.642	3.599	3.818, 3.989	3.578	
		103.95	73.71	75.34	79.69	75.64	61.24	57.91	
β -D-ManpA-(1→	20	4.670	3.988	3.659	3.738	3.670			
		101.06	71.28	73.56	69.45	76.58	176.48		
→4)- β -D-ManpA-OMe		4.590	4.032	3.756	3.949	3.726		3.540	
		101.90	70.58	72.51	79.54	77.38	175.89	57.73	
β -D-Galp-(1→	21	4.524	3.569	3.659	3.942	3.688	3.770, 3.794		
		103.88	72.00	73.56	69.55	75.94	61.84		
→4)-D-Glc-ol		3.651, 3.746	3.956	3.849	3.910	3.962	3.755, 3.863		
		63.61	72.89	70.60	80.55	72.37	63.06		
α -L-Rhap-(1→	22a	4.818	3.985	3.776	3.449	3.724	1.290		43
		101.50	70.87	71.14	72.91	69.39	17.31		
→6)- α -D-Glcp		5.218	3.537	3.717	3.398	3.946	3.724, 3.943		
		92.86	72.28	73.58	70.79	71.32	68.08		
α -L-Rhap-(1→	22b	4.828	3.979	3.782	3.448	3.732	1.295		57
		101.34	70.84	71.13	72.93	69.38	17.36		
→6)- β -D-Glcp		4.622	3.252	3.488	3.404	3.576	3.690, 3.988		
		96.76	74.97	76.57	70.69	75.60	67.88		
α -D-Manp-(1→	23a	4.907	3.991	3.846	3.680	3.696	3.775, 3.885		68
		100.52	70.86	71.53	67.79	73.61	61.91		
→6)- α -D-Manp		5.169	3.937	3.846	3.740	3.939	3.761, 3.961		
		95.01	71.60	71.37	67.79	71.68	66.99		
α -D-Manp-(1→	23b	4.914	3.992	3.849	3.681	3.702	3.771, 3.889		32
		100.54	70.84	71.51	67.79	73.59	61.91		
→6)- β -D-Manp		4.883	3.949	3.642	3.649	3.506	3.806, 3.925		
		94.67	72.03	74.08	67.54	75.26	66.99		
β -D-GlcpNAc-(1→	24	4.576	3.704	3.577	3.459	3.469	3.764, 3.939	2.042	
		102.23	56.46	74.69	71.02	76.75	61.77	23.04	175.22
→6)- β -D-Galp-OMe		4.294	3.514	3.632	3.908	3.770	3.808, 4.024	3.561	
		104.60	71.55	73.64	69.63	74.41	69.63	57.83	
L- α -D-Hepp-(1→	25	4.921	3.995	3.832	3.874	3.611	4.039	3.691, 3.744	
		101.40	70.79	71.67	66.97	72.32	69.74	63.87	
→7)-L- α -D-Hepp-OMe		4.772	3.932	3.761	3.861	3.545	4.177	3.712, 3.787	3.399
		101.84	70.68	71.65	66.91	72.16	68.18	69.82	55.53

^a $^1J_{\text{H1,C1}}$ in square brackets. ^b $^3J_{\text{H1,H2}}$ in parenthesis.

Table 3. ¹H and ¹³C NMR chemical shifts of trisaccharides in D₂O at 70 °C except for compounds **29** at 60 °C and **30** at 65 °C.

Trisaccharide	#	1	2	3	4	5	6	OMe	Me	C=O
β -D-Manp-(1→	26	4.778	4.046	3.653	3.613	3.395	3.762, 3.929			
		99.47	71.57	73.69	67.61	77.13	61.83			
→2)- α -D-Manp-(1→		5.160	4.283	3.874	3.707	3.761	3.774, 3.885			
		100.78	77.99	70.56	68.11	74.20	61.70			
→2)- α -D-Manp-OMe		4.957	3.983	3.881	3.693	3.603	3.778, 3.898	3.419		
		100.22	79.16	71.09	67.90	73.45	61.82	55.62		
α -D-Galp-(1→	27	5.166	3.848	3.902	4.016	4.065	3.721, 3.756			
		101.97	69.59	70.16	70.06	72.08	61.78			
→2)- α -D-Manp-(1→		5.260	4.011	3.921	3.796	3.918	3.794, 3.864			
		100.44	80.27	71.30	67.86	73.88	61.59			
→4)- α -L-Rhap-OMe		4.699	3.940	3.816	3.540	3.761	1.341	3.404		
		101.36	71.05	69.96	82.07	68.09	17.77	55.51		
α -L-Fucp-(1→	28	5.269	3.840	3.912	3.838	4.269	1.257			
		101.81	70.17	70.49	72.73	69.10	16.28			
→2)- β -D-Galp-(1→		4.589	3.708	3.871	3.948	3.729	3.789, 3.814			
		102.85	79.91	73.29	69.52	75.78	61.74			
→3)-D-GalNAc-ol		3.779, 3.792	4.396	4.107	3.547	4.142	3.660, 3.685		2.053	
		61.28	52.40	75.48	70.08	70.34	63.72		23.10	175.03
α -D-Glcp-(1→3)	29	5.125	3.706	3.834	3.499	4.032	3.781, 3.817			
		95.70	72.18	73.99	70.42	72.35	61.34			
→2,3)- α -L-Rhap-OMe		4.830	4.245	3.878	3.378	3.677	1.298	3.404		
		100.79	74.88	75.15	71.72	69.65	17.61	55.61		
β -D-GlcpNAc-(1→2)		4.828	3.751	3.444	3.457	3.428	3.751, 3.918		2.106	
		102.65	56.49	75.15	70.84	76.80	61.66		23.44	175.19
β -D-GlcpNAc-(1→3)	30	4.733	3.739	3.551	3.444	3.427	3.746, 3.918		2.044	
		103.50	56.68	74.97	71.08	76.72	61.87		23.08	175.21
→2,3)- α -L-Rhap-OMe		4.673	4.072	3.897	3.581	3.680	1.321	3.405		
		98.74	75.49	78.59	72.73	69.90	17.54	55.74		
α -D-GalpNAc-(1→2)		5.022	4.160	3.922	4.074	4.328	3.806, 3.806		2.056	
		96.08	50.80	68.40	69.36	71.30	61.81		22.88	175.26

Table 4. $^{13}\text{C}/^1\text{H}$ NMR chemical shifts from experiments, calculation by CASPER and assignments to pertinent atoms by CASPER for the O-antigens of the *Klebsiella* O5 polysaccharide, the *Shigella flexneri* X polysaccharide and the *Salmonella arizonae* O62 lipopolysaccharide.

<i>Klebsiella</i> O5 polysaccharide		<i>Shigella flexneri</i> X polysaccharide			<i>Salmonella arizonae</i> O62 lipopolysaccharide			
Experimental	Calculated	Assignment	Experimental	Calculated	Assignment	Experimental	Calculated	Assignment
						175.42	176.13	GalNAcA-6
						174.98	175.26	GalNAcA-CO
			174.58	175.01	GlcNAc-CO	174.46	174.72	GlcNAc-CO
101.47/5.34	101.29/5.33	ManI-1	102.37/4.81	102.07/4.86	GlcNAc-1	103.34/4.74	102.92/4.76	GlcNAc-1
100.79/5.16	100.72/5.17	ManIII-1	101.95/4.86	101.97/4.87	RhaIII-1	102.99/4.89	102.75/4.98	RhaIII-1
99.29/4.79	99.33/4.76	ManII-1	102.00/5.10	101.90/5.13	RhaI-1	101.69/5.17	101.64/5.16	RhaII-1
81.19/3.73	81.25/3.74	ManII-3	101.45/5.16	101.64/5.16	RhaII-1	100.63/5.03	100.95/4.96	RhaIV-1
79.28/4.12	79.10/4.13	ManI-2	95.58/5.16	95.70/5.12	Glc-1	99.69/4.97	99.56/5.00	RhaI-1
78.06/4.28	77.96/4.29	ManIII-2	82.53/3.50	82.76/3.52	GlcNAc-3	95.80/5.14	95.81/5.11	GalNAcA-1
77.03/3.43	77.22/3.43	ManII-5	79.22/4.05	79.08/4.10	RhaII-2	82.46/3.64	82.58/3.62	GlcNAc-3
74.21/3.73	74.09/3.73	ManIII-5	78.22/3.77	78.72/3.79	RhaIII-3	80.47/3.81	79.78/3.80	RhaIV-2
74.23/3.78	74.08/3.76	ManI-5	76.89/3.43	76.83/3.45	GlcNAc-5	78.73/4.07	79.08/4.10	RhaII-2
71.39/4.17	71.10/4.17	ManII-2	74.92/3.93	74.96/3.97	RhaI-3	79.06/3.93 ^a	78.94/3.93	RhaI-3
70.97/4.01	70.89/4.01	ManI-3	75.10/4.39	74.93/4.39	RhaI-2	78.67/3.83	78.69/3.87	RhaIII-3
70.63/3.87	70.52/3.88	ManIII-3	74.10/3.82	73.99/3.83	Glc-3	76.66/3.43	76.75/3.45	GlcNAc-5
68.00/3.72	67.90/3.74	ManIII-4	73.21/3.46	73.09/3.51	RhaII-4	75.60/4.33	75.50/4.27	RhaI-2
68.00/3.72	67.80/3.72	ManI-4	72.38/4.02	72.35/4.03	Glc-5	73.29/3.47	73.09/3.51	RhaII-4
67.01/3.73	66.85/3.74	ManII-4	72.29/3.71	72.18/3.70	Glc-2	73.21/3.47	73.06/3.46	RhaIV-4
61.85/3.92	61.66/3.89	ManI – 6a	72.49/3.53	72.15/3.57	RhaIII-4	72.47/3.57	72.56/3.60	RhaI-4
61.85/3.77	61.66/3.75	ManI – 6b	71.78/3.36	71.50/3.43	RhaI-4	72.47/3.57	72.28/3.60	RhaIII-4
61.81/3.94	61.63/3.93	ManII – 6a	71.47/3.84	71.33/3.88	RhaIII-2	72.21/4.81	71.99/4.68	GalNAcA-5
61.81/3.78	61.63/3.76	ManII-6b	70.90/3.91	70.91/3.97	RhaII-3	70.80/3.88	70.94/3.83	RhaIV-3
61.66/3.86	61.56/3.86	ManIII – 6a	70.59/3.48	70.42/3.50	Glc-4	70.92/3.95	70.91/3.97	RhaII-3
61.66/3.83	61.56/3.77	ManIII-6b	70.33/3.72	70.21/3.76	RhaI-5	70.90/4.12	70.75/4.15	RhaIII-2
			69.90/3.74	69.97/3.81	RhaII-5	69.82/4.36	70.53/4.41	GalNAcA-4
			69.88/4.00	69.93/4.01	RhaIII-5	70.38/3.73	70.50/3.76	RhaI-5
			69.48/3.51	69.52/3.51	GlcNAc-4	70.04/3.79	70.04/3.82	RhaIII-5
			61.80/3.86	61.45/3.93	GlcNAc – 6a	70.04/3.79	69.97/3.81	RhaII-5
			61.80/3.75	61.45/3.76	GlcNAc-6b	69.89/3.98	69.96/3.95	RhaIV-5
			61.43/3.82	61.34/3.80	Glc-6b	70.29/3.36	69.76/3.50	GlcNAc-4
			61.43/3.75	61.34/3.80	Glc – 6a	68.04/4.01	67.72/4.04	GalNAcA-3
			56.24/3.85	56.06/3.87	GlcNAc-2	62.31/3.92	61.66/3.93	GlcNAc – 6a
			23.44/2.09	23.42/2.12	GlcNAc-Me	62.31/3.68	61.66/3.76	GlcNAc-6b
			17.58/1.30	17.50/1.30	RhaII-6	56.85/3.71	56.25/3.85	GlcNAc-2
			17.65/1.23	17.46/1.26	RhaI-6	50.41/4.17	50.34/4.20	GalNAcA-2
			17.29/1.25	17.16/1.26	RhaIII-6	23.44/2.07	23.06/2.05	GlcNAc-Me
						22.92/2.05	22.88/2.06	GalNAcA-Me
						17.68/1.30	17.67/1.35	RhaI-6
						17.55/1.30	17.50/1.30	RhaII-6
						17.61/1.30	17.49/1.25	RhaIV-6
						17.55/1.30	17.21/1.30	RhaIII-6

^a Cross-peak not visible in Figure 6b. See text for details.